DNA Bending Stiffness on Small Length Scales

Chongli Yuan,[1] Huimin Chen,[2] Xiong Wen Lou,[1] and Lynden A. Archer[1]
[1]School of Chemical and Biomolecular Engineering, Cornell University, Ithaca, New York 14853, USA
[2]Department of Applied and Engineering Physics, Cornell University, Ithaca, New York 14853, USA
(Received 16 April 2007; published 7 January 2008)

Bending properties of short (15–90 bp), double-stranded DNA fragments are quantified using fluorescence resonance energy transfer and small angle x-ray scattering. Results from both types of measurements indicate that short double-stranded DNA fragments exhibit surprisingly high flexibility. These observations are discussed in terms of base-pair-level length fluctuations originating from dynamic features of Watson-Crick base pairs.

DOI: 10.1103/PhysRevLett.100.018102 PACS numbers: 87.14.G−, 87.10.−e

DNA from a single human cell has a contour length of 1.8 m and is composed of billions of Watson-Crick base pairs, unit length 0.34 nm. This DNA must simultaneously fit within the cell nucleus, diameter 1–5 μm, and be packaged in such a way that the genetic information it encodes is accessible to the cell's transcription machinery. To achieve these requirements, DNA molecules are packaged in highly organized modular structures known as nucleosomes, in which the molecules are bent, twisted, and stretched around histone octamer proteins with average diameters around 13 nm [1]. The physicochemical factors that control nucleosome formation and regulate its stability are of fundamental interest to physical scientists and biologists because they are believed to be central for understanding DNA templated processes in the cell [2].

A 147 bp DNA fragment is generally involved in forming the fundamental unit of the nucleosome, namely, the nucleosome core particle. A much smaller DNA segment length [O(10 bp)] bridges neighboring binding sites on the histone [1], and is subjected to significant conformational constraints. The mechanical properties of DNA on nanometer length scales are therefore an important determinant of how DNA fragments accommodate these constraints. Current understanding of mechanical properties of DNA molecules is largely derived from experiments using micron-size DNA, and discussed in terms of simple statistical mechanical models, e.g., the wormlike chain model. Several new experimental tools are available that allow mechanical properties of DNA to be probed on smaller length scales, comparable to those on which it is distorted in nucleosomes. These emerging tools make it possible to pose and answer new questions about the fine-scale structure, conformation, and bending properties of nucleic acids on the nanometer scale [3,4].

The cyclization assay is a biochemical tool widely used to quantify bending properties of DNA molecules. In this method DNA with ligatable, ''sticky'' ends is trapped into rare, highly bent conformations by ligase, allowing the population of bent states to be isolated and counted. Recent results using this method indicate that the bending stiffness of double-stranded DNA (dsDNA) with sizes $<$100 bp can be as much as 3–5 folds lower than anticipated from statistical mechanical models such as the wormlike chain [5,6]. Various approaches have been employed to identify the origin of this large discrepancy [7–9]. While there is still no conclusive answer, a breakdown of the continuum model [8,9] and possible experimental artifacts [7] are the most common explanations for the experimental observations. There is nonetheless growing evidence that as DNA fragment size approaches nanometer dimensions, new approaches are needed to understand their mechanical properties [10–12].

In this Letter we report results obtained using two different methods for measuring the bending stiffness of dsDNA with sizes ranging from 10–90 bp. Both techniques allow bending properties of dsDNA to be probed without interference from other biological molecules. Significantly, they lead to the conclusion that the bending stiffness of dsDNA molecules on small length scales is significantly lower than expected.

The wormlike-chain (WLC) model has been extensively used to characterize bending properties of dsDNA fragments. In this model, intermolecular interactions are coarse grained in terms of the constraints connected segments impose on the orientation of connecting bonds. Strictly speaking, the WLC model is applicable only to polymers that are long compared to their persistence length; it is nonetheless informative to use it as a tool for analyzing bending properties of shorter molecules. For dsDNA, a bending potential determines the equilibrium distribution of angular displacements (θ) between neighboring segments. The persistence length can be written as $L_p = \frac{l(1+\langle\cos\theta\rangle)}{2(1-\langle\cos\theta\rangle)}$, where l is the segment length [7]. If the bending energy assumes a quadratic form, the conformation properties for relatively long dsDNA segments are approximated well using this model [7], with a persistence length in the range 40–50 nm, depending on the ionic strength of the medium.

The bending stiffness of dsDNA can be quantified from the end-to-end distance distribution using fluorescence resonance energy transfer (FRET). By reporting the distance between two fluorescing labels, i.e., donor and ac-

ceptor, attached to the ends of the target molecule via a short *linker* polymer, FRET acts as a very sensitive ruler for measuring the end-to-end distance. The energy transfer efficiency $E \equiv 1 - \frac{\tau_{da}}{\tau_d}$ is related to the separation R of donor and acceptor by $E = 1/[1 + (R/R_0)^6]$. τ_d and τ_{da} are fluorescence lifetime of the donor in absence and presence of the acceptor, and R_0 is the Förster radius [5.0 nm for the 6-FAM/TAMRA (6-fluorescein/tetramethyl rhodamine) pair [13]]. In our experiments, the energy transfer efficiency is measured using a time-dependent scheme, which allows both the average end-to-end distance and variance to be determined [14].

The detailed experimental setup and analysis procedure used to recover moments of the end-to-end distance distribution for *end-labeled* DNA, $P(r) = \frac{1}{\sigma_m\sqrt{2\pi}} \exp[-\frac{1}{2}(\frac{\bar{r}-r}{\sigma_m})^2]$ ($\bar{r}$, σ are the mean end-to-end distance and variance), from FRET data are discussed in detail in Refs. [13,14]. Because the DNA fragments are end-labeled using a short, but flexible linker polymer, the variance (σ_m) deduced from the FRET experiment includes information about fluorophore-DNA "bond" length fluctuations (σ_r), as well as about the intrinsic bending flexibility (σ_e) of dsDNA. σ_r can be determined from length-dependent FRET studies, and for short dsDNA fragments, it can be easily shown that $\sigma_m^2 \simeq \sigma_r^2 + \sigma_e^2$, with a relative error no more than 10%. σ_e can be related to the contour length L as $\sigma_e = \frac{L^2}{L_p\pi^2}$, based on "Euler instability" [15].

Figure 1 shows that a plot of σ_m^2 against L^4 is indeed a straight line for the smallest fragments; its slope yields an apparent persistence length $L_p = 11 \pm 2$ nm. Before discussing the significance of this result, we first evaluate its reliability. Inaccuracy of the Förster radius R_0, for example, can lead to systematic errors in the value of L_p deduced from FRET. To minimize this effect the DNA sequences used in the study (see Table I) were deliberately designed so that the bases adjacent to the fluorescence linkage are the same for all fragment lengths. This choice eliminates any potential length dependence of the Förster radius. The accuracy of R_0 can also be independently determined from the average end-to-end distance, which yields no more than a 5% relative error in L_p.

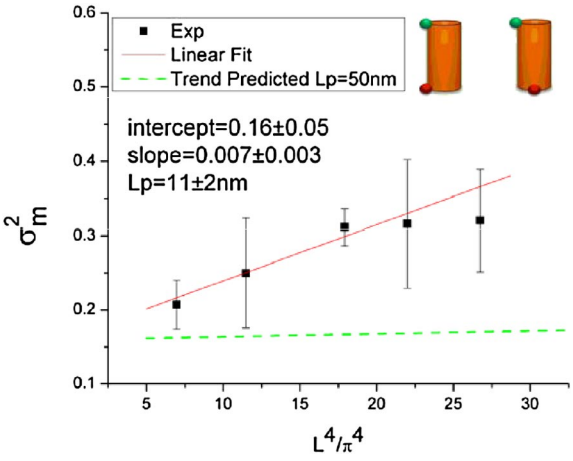

FIG. 1 (color online). σ_m^2 of short DNA fragments, 15–21 bp, versus DNA contour length. Measurements were performed at room temperature in aqueous solutions containing 10 mM Tris-HCl, 500 mM NaCl, 1 mM EDTA, *p*H 8.0.

Care is also needed to eliminate spurious contributions to the measured FRET efficiency from contamination by more flexible single-stranded DNA fragments. This effect can be minimized using two approaches: a high salt concentration and complimentary, nonfluorescently labeled oligos as in Ref. [13]. The effectiveness of the first procedure was evaluated by carrying out FRET measurements in buffers with different salt concentrations. As the salt concentration is gradually lowered below 50 mM, large increases in variance are observed for the shorter DNA fragments, consistent with destabilization of the dsDNA. However, even at 50 mM the σ_m^2 vs L^4/π^4 line is robust enough for the shortest dsDNA fragments to extract the persistence length, $L_p 18 \pm 3$ nm, which is again substantially lower than the consensus estimate. Finally, the finite diameter of the DNA (see inset of Fig. 1) cannot be ignored for the short fragments considered here. This effect can be captured by taking into account the range of phasing angles taken by the two fluorescent molecules; i.e., 10.5 bp corresponds to a complete helix turn. If the fluorescence-DNA bond is completely flexible, the modified persistence length is 12 ± 3 nm; if bond rotation is partially hindered, it is 13 ± 3 nm.

Small-angle x-ray scattering (SAXS) provides a complimentary method for quantifying the bending stiffness of short dsDNA. Unlike FRET which can provide information about the end-to-end distance distribution, SAXS data provide more limited, but very accurate, information about the radius of gyration (R_g) of small molecules at nanometer length scales. We select DNA fragment with sizes of 16, 21, 66, and 89 bp and the sequences specified in Table I for these measurements. DNA sample preparation and the

TABLE I. DNA sequences used in this study, "*" identifies fragments with 5′ ends labeled with 6-FAM and 3′ labeled with tetramethylrhodamine, for FRET.

DNA length	Sequence
15 bp*	CGA CTC CAG GTC ACC
16 bp	GGA CTC CAG GTC ACC C
17 bp*	CGG ACT CCA GGT CAC CC
19 bp*	CGG GAC TCC AGG TCA CCC C
20 bp*	CGG GAC TCC AGG TCT ACC CC
21 bp*	CGA CTC TGC CAG CGG TCA CCC
66 bp	CCA GTG TGC AGG GTG GCA AGT GGC TCC TGA CCT GGA GTC TTC CAG TGT GAT GAT GGT GAG GAT GGG
89 bp	GGT CGT ACT AAC TCG AGA TAA CAC GGC CAA CAG CAC AGG GGA TCA GCA CCG TGG AGG CGA TAA ATA AAA GTA GTT CTA CGC AGC CGG CC

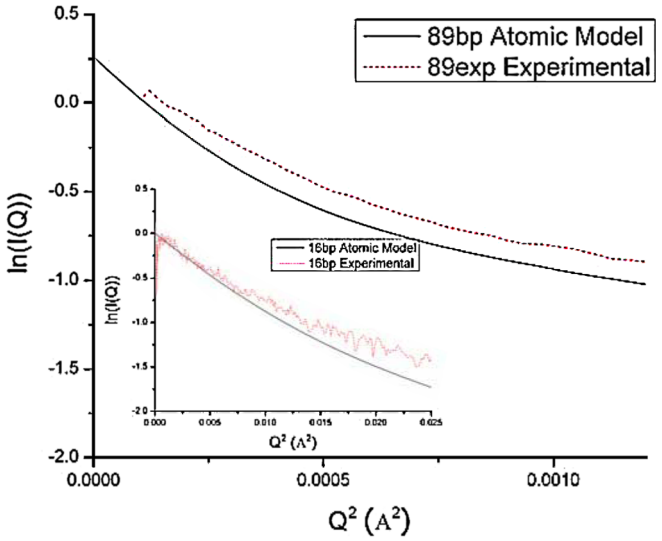

FIG. 2 (color online). Plot of $\ln(I(q))$ vs q^2 for 16 and 89 bp dsDNA.

beam line setup at the Cornell High Energy Synchrotron Source (CHESS) are described in detail in Refs. [16,17]. The R_g values can be readily calculated using the Guinier function, $I(q) = \exp(-\frac{q^2 R_g^2}{3})$, at low scattering angles or using an inverse-transform method, e.g., GNOM [18]. R_g can be related to the persistence length as $\langle R_g^2 \rangle = \frac{1}{3} L L_p - L_p^2 + \frac{2L_p^3}{L} - \frac{2L_p^4}{L^2}[1 - \exp(-\frac{L}{L_p})]$ [19]. R_g values obtained in this way are compared with those obtained from the scattering data in Table II. The table also includes R_g predicted by the WLC assuming persistence lengths of 50 and 20 nm, respectively. It is apparent from the table that the WLC with $L_p = 20$ nm more consistently predicts the measured R_g. These results therefore also indicate that under the experimental conditions, dsDNA is more flexible than expected. Again, before discussing the possible physical origin of the results we consider potential sources of error. It is well known that the presence of A tracts can alter the bending stiffness of dsDNA. None of the dsDNA sequences examined here contain these repeats. The 89 bp fragment, however, derives from nucleosome positioning sequence as in Ref. [6], which could make it more flexible than a random dsDNA sequence.

Access to sufficiently low scattering angles in SAXS experiments is also always a concern for measuring R_g of long DNA fragments. Errors produced by this effect can be eliminated by comparing the scattering function predicted using atomistic models for DNA [17] with that obtained experimentally over a large q range. As illustrated in Fig. 2, the scattering data manifest significant positive deviations from the model predictions for both the short and long dsDNA fragments, confirming the higher flexibility deduced on the basis of the R_g values. The metal ions surrounding the DNA surface can also contribute to the measured x-ray scattering. This has the effect of overestimating the size of DNA, and thus would be resolved as an underestimation of DNA bending flexibility.

The experimental results from FRET and SAXS measurements therefore indicate that short dsDNA molecules are more flexible than anticipated from previous analyses of larger fragments. A similar result has been reported for short DNA fragment by Shroff *et al.*, using an optical force sensor [12]. The origin of the extra flexibility on small length scales is an important question of broad scientific interest. To account for more frequent spontaneous large-angle bends at small length scales, Wiggins and Nelson proposed that the bending energy of dsDNA is of the form $E(\theta) = \alpha|\theta|k_B T$ [10,20], where α is a constant that varies with the segment length [10]. This model implies a breakdown of the continuum model for DNA mechanics on small length scales. The apparent softening we observe from FRET and SAXS experiments could be interpreted using this new expression, with α obtained by fitting the model to data. A drawback of this approach is that it does not reveal the physical origin of the apparent softening of short dsDNA.

One possibility is that the softening originates from dynamic features of Watson-Crick base pairs, e.g. *base flipout* or *base-pair breathing*. The probability of one nucleotide spontaneously unpairing (''flipping out'') from its complement in the helix can be calculated using the free energy change associated with the hydrogen bonds, 2–$5 k_B T$, where the large range is due to a dependence on the detailed DNA sequence context [21]. The base flipout probability (P_{fl}) can therefore range from 10^{-2} to 10^{-3}, implying that a short DNA fragment containing N base pairs can on average contain $10^{-2}N$ to $10^{-3}N$ local defects. The base-pair flipout process has been extensively

TABLE II. Comparisons of R_g data from SAXS with predictions based on the rigid-rod and wormlike-chain models. The WLC prediction is corrected for the finite diameter of DNA using the formula $R_{g,\mathrm{pred}}^2 = R_{g,\mathrm{WLC}}^2 + R_{\mathrm{DNA}}^2/2$, where $R_{\mathrm{DNA}} = 1$ nm.

DNA length (bp)	R_g (nm), (measured, Guinier analysis)	R_g (nm), (measured, inverse transform)	R_g (nm), (predicted, rigid cylinder)	R_g (nm), (predicted, $L_p = 50$ nm)	R_g (nm), (predicted, $L_p = 20$ nm)
16	1.66 ± 0.02	1.66 ± 0.02	1.72	1.71	1.68
21	2.03 ± 0.02	2.11 ± 0.03	2.18	2.15	2.11
66	6.00 ± 0.20	6.04 ± 0.10	6.52	6.24	5.88
89	6.80 ± 0.09	7.74 ± 0.20	8.76	8.27	7.65

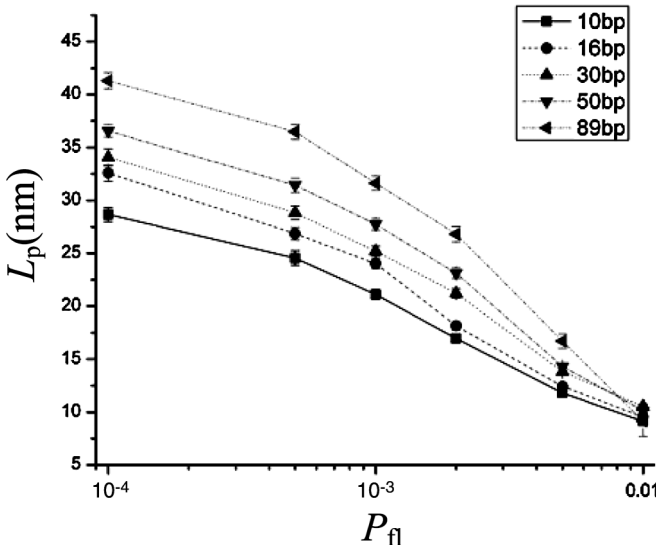

FIG. 3. Simulated persistence length (L_p) calculated as a function of nucleotide flipout probability (P_{fl}) using Monte Carlo simulation with a 30° kink angle per flipped-out base [13].

studied using NMR [22,23] and other chemical methods [24,25]. These methods suggest that flipout occurs on millisecond time scales. The equilibrium constant obtained from NMR experiments is in the range of 10^{-5}–$10^{-6}/\alpha'$ ($0 < \alpha' < 1$), where α' is a so-called accessibility parameter. In a previous FRET study we explored the effect of deliberately introduced base-pair defects on the average end-to-end distance and flexibility of dsDNA. These results indicate that a single unpaired base produces an approximately 30° kink in the DNA backbone [13].

To sketch out how this effect might influence the persistence length of short dsDNA, we use a Monte Carlo (MC) method to generate trajectories of 10 000 molecules with bending energy $E(\theta) = \frac{1}{2}k_BT(\frac{\xi}{l})\theta^2$ and flipout possibility P_{fl}; $\xi = 50$ nm, $l = 2 \times 0.34$ nm. The simulated end-to-end distance distribution is of the form $P(x) = \frac{L}{\sigma_e} \times \exp(-\frac{(L-x)}{\sigma_e})$, allowing σ_e, and thereby L_p to be determined. By implementing the kink angle criterion observed in the earlier experiments [13], the effect of kink magnitude on the simulated persistence length can be readily evaluated. To ensure that the results are insensitive to the simulated system size, larger number of trajectories were tested and found to have no effect on the simulated persistence length. Figure 3 summarizes the results from the MC simulations. Once the flipout mechanism is triggered, L_p drops sharply from the input persistence length of 50 nm. When $P_{\mathrm{fl}} \ll 1/N$, the simulated L_p is a relatively weak function of P_{fl}, but manifests an approximately inverse dependence on the length of the DNA fragment. This implies that the dsDNA will appear to be softer as its length decreases. At even higher values of P_{fl} [O (10^{-2})] this trend gradually disappears and much lower L_p values are observed, irrespective of the size of the dsDNA fragment. The results are consistent with our hypothesis that the apparent reduction in L_p deduced from the FRET and SAXS data can be understood in terms of spontaneous unpairing of bases.

In conclusion, we have used FRET and SAXS to quantify the bending properties of short dsDNA. We find that the apparent persistence length is substantially lower than the consensus value for dsDNA. A coarse-grained WLC model incorporating base-pair-level length fluctuations is simulated using a MC technique. This model indicates that rare base-pair level flipout events contribute significantly to mechanical properties of short dsDNA.

This study was supported by the National Science Foundation, DMR0551185. We are grateful to Xiangyun Qiu for assistance with SAXS, and to Donald L. Koch for enlightening discussions.

[1] T. J. Richmond and C. A. Davey, Nature (London) **423**, 145 (2003).
[2] P. G. Giresi, M. Gupta, and J. D. Lieb, Curr. Opin. Genet. Dev. **16**, 171 (2006).
[3] C. Bustamante, J. F. Marko, E. D. Siggia, and S. Smith, Science **265**, 1599 (1994).
[4] P. J. Hagerman, Annu. Rev. Biophys. Biophys. Chem. **17**, 265 (1988).
[5] T. E. Cloutier and J. Widom, Mol. Cell **14**, 355 (2004).
[6] T. E. Cloutier and J. Widom, Proc. Natl. Acad. Sci. U.S.A. **102**, 3645 (2005).
[7] Q. Du, C. Smith, N. Shiffeldrim, M. Vologodskaia, and A. Vologodksii, Proc. Natl. Acad. Sci. U.S.A. **102**, 5397 (2005).
[8] J. Yan and J. F. Marko, Phys. Rev. Lett. **93**, 108108 (2004).
[9] P. A. Wiggins, R. Phillips, and P. C. Nelson, Phys. Rev. E **71**, 021909 (2005).
[10] P. A. Wiggins *et al.*, Nature Nanotechnology **1**, 137 (2006).
[11] G. S. Manning, Biophys. J. **90**, 3208 (2006).
[12] H. Shroff *et al.*, Nano Lett. **5**, 1509 (2005).
[13] C. Yuan, E. Rhoades, X. W. Lou, and L. A. Archer, Nucleic Acids Res. **34**, 4554 (2006).
[14] S. L. Williams, L. K. Parkhurst, and L. J. Parkhurst, Nucleic Acids Res. **34**, 1028 (2006).
[15] J. Wilhelm and E. Frey, Phys. Rev. Lett. **77**, 2581 (1996).
[16] R. Das *et al.*, Phys. Rev. Lett. **90**, 188103 (2003).
[17] X. Qiu, L. W. Kowk, H. Y. Park, J. S. Lamb, K. Andresen, and Pollack, Phys. Rev. Lett. **96**, 138101 (2006).
[18] Downloaded from http://www.embl-hamburg.de/ExternalInfo/Research/Sax/gnom.html.
[19] M. Rubinstein and R. Colby, *Polymer Physics* (Oxford University, New York, 2002), 1st ed.
[20] P. A. Wiggins and P. C. Nelson, Phys. Rev. E **73**, 031906 (2006).
[21] J. SantaLucia and D. Hicks, Annu. Rev. Biophys. Biomol. Struct. **33**, 415 (2004).
[22] M. Leijon and Gräslund, Nucleic Acids Res. **20**, 5339 (1992).
[23] C. Cao, Y. L. Jiang, J. T. Stivers, and F. Song, Nat. Struct. Mol. Biol. **11**, 1230 (2004).
[24] M. A. Spies and R. L. Schowen, J. Am. Chem. Soc. **124**, 14 049 (2002).
[25] L. L. O'Neil and O. Wiest, J. Am. Chem. Soc. **127**, 16 800 (2005).